APPRAISAL OF PHOTOVOLTAIC CELL TECHNOLOGIES AND SEASONAL PERFORMANCE AND OPERATIONAL VIABILITY: A STUDY IN DURBAN, SOUTH AFRICA

EBHOTA W., TABAKOV P.
Department of Mechanical Engineering, Institute for Systems Science, Durban University of Technology, Durban, South Africa.
ebhotawilliams1@gmail.com

Abstract - This study analyses the PV potential in Mountain Rise, Durban, South Africa, considering three PV panel technologies and tilt angles in a 20-kWp PV system (c-Si, CdTe, and CIS cells; tilts of 30°, 10°, and 48° for year-round, winter, and summer conditions, respectively, with a fixed Azimuth of 0°). Computational modelling with Solargis Prospect, pvPlanner, and PV*SOL is utilized. Findings reveal the site's annual GHI (1636 kWh/m2) is lower than GTI at different tilts (30° = 1839.3 kWh/m2, 10°/48° = 1921 kWh/m2). Average ambient conditions include temperature (20.8 °C), wind speed (4.6 m/s), and relative humidity (78%). Transitioning from GHI to GTI yields a 12% irradiance increase at βopt (30˚) and 15% at βwin/βsum (10˚/48˚). PV system performance in MWh at βopt is 30.3, 28.7, and 28.2 for CdTe, CIS, and c-Si, respectively, while at βwin/βsum, it is 32.1, 30.7, and 29.9. Average PR values in winter are 82.9%, 80%, and 78.8%, and in summer, they are 83.7%, 78.1%, and 76.9%. The study concludes that CdTe is the most technically viable PV cell, and a season-based tilt approach enhances electricity generation. Additionally, deploying PV systems of CdTe, CIS, and c-Si prevents CO2 emissions of 10,377, 10,409, and 11,082 kg/year, respectively.

Keywords: Photovoltaic potential season-based assessment; Solar irradiation; Solar photovoltaic; Photovoltaic system performance; Photovoltaic system computational modelling.

1. INTRODUCTION

In recent times, there has been a significant increase in global energy demand, accompanied by pressing concerns related to both the environment and human health. This surge in energy needs is primarily a result of various socio-economic development activities driven by factors such as rapid population growth, industrialization, and urbanization. These activities encompass activities like deforestation for fuel, fossil fuel extraction and consumption, cement production, cooking, and the transportation of goods [1-4]. Unfortunately, these activities also result in the emission of harmful greenhouse gases (GHGs) that exacerbate climate change. It's worth noting that this trend of socio-economic development shows no signs of slowing down, and it's expected to be most pronounced in the Global South, particularly in regions like sub-Saharan Africa (SSA) and Asia [5, 6]. The energy demand is a fundamental requirement for socio-economic development, and its sustainability hinges on access to adequate energy sources [7]. Fossil fuels have historically played a pivotal role in meeting this demand, driving the growth of large economies and supporting rapid economic development in developing countries worldwide [8]. However, increased energy consumption comes with consequences, including higher GHG emissions, increased health problems, and the exacerbation of climate change. Notably, the energy sector is the largest contributor to global CO_2 emissions, with biomass fuels being extensively used in SSA.

Beyond environmental concerns, the Global South continues to grapple with persistent issues related to inadequate and unreliable power supply due to various inhibiting factors such as insufficient funds, technical expertise, and political will. This energy demand is expected to sustain the consumption of fossil fuels and the resultant GHG emissions, particularly CO2. To address these challenges, the United Nations (UN) and its affiliated organizations are actively pursuing a transition to a net-zero-CO_2 economy. This involves reducing fossil fuel consumption and shifting towards cleaner energy sources [9, 10]. Consequently, the UN is advocating for greater development and deployment of sustainable energy systems that can enhance energy security, accessibility, and affordability. To adequately tackle these complex issues, it is essential to implement integrated policies, comprehensive plans, and suitable energy generation and distribution technologies in these regions.

Socio-economic development comes with adverse conditions that need mitigation and management initiatives. Since energy is a basic essential for human survival, alternative energy sources that meet modern energy requirements need to be identified. The alternative energy sources, which are regional-based, should be assessed for both technical and economic feasibility before development and deployment. The alternative energy sources considered the most appropriate [5, 11-14] that are receiving attention and are being developed for deployment are geothermal, tidal,

hydropower, solar, wind, and biomass. However, these alternative sources are regional and seasonal dependent; and are associated with cost estimation complexity. Other challenges are system design difficulty, energy intermittency, low power density in supply, and difficulty in large-scale (RE) generation [15, 16]. This has led to the development of several RE design software applications for more accurate results in a shorter time [17-19].

Amongst the RE resources, solar photovoltaic (PV) is the fastest-growing RE technology globally [20]. Photovoltaic is a phenomenon, where electrical energy is generated from certain materials that absorb photons when exposed to the sun and this was first observed early in the 19th century [21]. The sun is about 150 million km away from the earth, approximately 1.4 million km in diameter, and emits energy average at a rate of $3.8x10^{23}$ kW/s daily [22]. Nuclear fusion reactions near its core supply solar energy that is estimated to continue for about several billion years. Energy scarcity in the Global South and the continuous consumption of fossil fuels globally and its consequences can be over if the enormous amount of energy coming from the sun is adequately harnessed. Merits such as lack of CO_2 emissions, widespread availability, generated anywhere (decentralized system), reduction in transmission losses, and the possibility of modular systems are associated with solar PV systems. Others are the creation of more jobs per unit of electricity production compared to fossil fuels and lowering costs of PV system's components and projects. With the impacts of the climate change crisis increasingly being felt in our daily lives, relying on renewable sources for energy is growing rapidly. This trend of producing clean energy appears to be a path of no return as it facilitates CO_2 emission reduction.

The call for the utilisation of PV technology to meet energy demand for socio-economic growth and CO_2 emissions reduction is now more compelling. This is due to the uncertainties surrounding fossil fuels, such as depletion, unstable prices, subsidies, and their disposition as a tool for economic war. For optimal use of PV systems, several factors that influence PV performance need to be studied and understood. These factors include solar irradiation, PV cells, wind energy, shading effect, season and geographical location, soiling factor, and cell temperature. A lot has been achieved in the development of solar PV technology but several research gaps still exist, including the evaluation of PV cell technologies and systems concerning seasonal performance and operational viability. This study is expected to enhance the performance of PV systems through the considerations of seasonal variations, operational optimisation, environmental impact, technological advancements and economic viability.

It is noteworthy that previous studies [23, 24] on PV system design and performance prediction through computational modelling typically employed a simplified approach. This approach considers an optimal tilt angle all year round and this optimal tilt does not account for the seasonal variations. Therefore, this study aims to analyse the influence of seasonal fluctuations in the performance of solar PV systems utilising two categories of PV cell technologies. The two categories of PV cells to be considered are first-generation (monocrystalline silicon (mono-c-Si)), and second-generation (cadmium telluride (CdTe) and copper indium selenide (CIS)). In the evaluation of system performance, different tilt angles will be utilised for all year-round, winter, and summer seasons. The research will be conducted hypothetically at a designated site along Mountain Rise Road in Durban, South Africa. While this study primarily focuses on assessing PV system performance, it is essential to emphasise that an initial assessment of PV potential is a prerequisite in this process. Hence, this study provides answers to the meteorological and PV performance research questions based on all year-round, winter, and summer seasons and PV cells, such as what the – annual sum of global horizontal irradiance (GHI) and global tilt irradiance (GTI) at different tilts, annual average ambient PV system conditions, the electricity generation of different PV cell systems at various tilt, the average PR for the different PV cell systems, and annual avoidable CO_2 emissions by c-Si, CdTe, and CIS PV cell systems deployments.

2. STUDY BACKGROUND

Solar energy is caused by the energy released during the collision of photons (tiny particles) carried by the sun's rays and the atoms on their paths. This accounts for the warmth felt by the skin when exposed to the sun, as the collision of photons from the sun and the atoms in the skin produces heat. In this context, special materials (semiconductors), such as silicon and CdTe trap photons once sun rays strike them and this interaction produces electricity instead of heat. This conversion process of electricity production by the semiconductor, called PV, involves the generation of a flow of electrons (electricity) from the absorbed photons received from the sun. Hence, irradiation and solar PV cells are the most crucial components that must be present in a solar system to produce PV energy. Irradiation is the primary source of raw energy that solar PV cells convert into electricity, and this makes them dependently linked to solar PV system components. They are integral parts of the process that provides a sustainable, renewable, and environmentally friendly source of electricity that reduces GHG emissions, promotes energy independence, and contributes to economic development. Solar PV technology is expected to continue growing in the global energy mix.

2.1. Overview: Solar PV cell technologies

A PV system, which is becoming one of the most deployed RE technologies globally, has PV cells as the most significant part. Over decades of development, through the instrumentality of materials and production systems, PV cells have evolved into three generations - first, second, and third generations.

2.1.1. First-generation solar cells

The commonest commercially available PV cell, the c-Si, with a performance conversion efficiency range of

15% to 20% belongs to the first-generation cells. They dominate the rooftop PV panels market and makeup about 80% of the PV panels sold globally [25]. They are relatively high in stability and performance [26]. Based on the silicon deployed, first-generation PV cells can be categorised into PV cells three as follows - crystalline silicon (c-Si) and hybrid silicon.

Crystalline silicon – currently, there are two types of c-Si in the market and there are monocrystalline (mono-c-Si) and polycrystalline (poly-c-Si) PV panels. This set of PV cells is among the most efficient, oldest, and most reliable methods of generating electricity from sunlight. The mono-c-Si are the commonest and easiest to recognise due to their dazzling blue or black colour [27]. They are relatively more efficient and expensive compared to poly-c-Si and thin-film PV panels. The complex process involved in growing large pure silicon crystals and the energy-intensive process required to produce mono-c-Si accounts for the high cost. A monocrystalline PV module is made from a single silicon crystal, developed carefully under well-defined conditions. Elevated temperatures influence the PCE of c-Si cells inversely as shown by empirical and theoretical studies [28-30]. They perform optimally (i.e. PCE between 15% and 20%) at an ambient temperature of 25 °C or below [31]. However, the world's most efficient commercially available monocrystalline PV panels of 24.2% PCE were produced by SunPower (USA) in 2010 [32].

2.1.2. Second Generation of Solar Cells

Amorphous silicon, cadmium telluride (CdTe), and copper indium gallium selenide (CIGS), sometimes called copper indium selenide (CIS), belong to the second-generation PV cells. The range of PCE of CdTe PV cells is 10% to 15% [33]. The flexible thin-film PV cells that are members of this generation are cheaper due to their fast and inexpensive manufacturing processes that consume fewer raw materials. Cadmium telluride PV cell is the second most commonest PV technology after c-Si and has a laboratory PCE record of 22.1% [34] and accounts for 5% of the global market [35].

3. METHOD

Having access to accurate solar irradiation data for a site is a crucial prerequisite for a dependable study of potential and system performance prediction. Notably, in the context of the global south, there is a notable deficiency in the availability of irradiation databases. Traditionally, spectral pyranometers have been employed to compute the global solar radiation at specific locations by installing these devices at various points within a region. Nevertheless, this approach comes with substantial demands, including the need for frequent cleaning, maintenance, and calibration of the sensors. Additionally, it involves filtering, examining, and smoothing the recorded data, making it a labour-intensive and time-consuming process that is susceptible to errors. A more cost-effective and convenient alternative is to employ climatological parameters for the calculation of global solar radiation without introducing errors.

In this study, computational modelling using the Solargis, PVsyst and PV*SOL applications was employed to obtain irradiation data for the site location, and this irradiation data is discussed in this section. To conduct this study effectively, the study situated a hypothetical 20-kilowatt peak (kWp) grid-connected PV system in Mountain Rise, Durban, South Africa. To analyse the PV system's performance, the study recognised four distinct seasons in Durban - Winter (June to August), Spring (September to October), Summer (November to March), and Autumn (April to May). However, due to meteorological data limitations of these seasons, two categories of seasons were adopted: Winter (April to September) and Summer (October to March). To evaluate the PV system's potential, the study determined the site's geographical coordinates (latitude and longitude) and utilised these coordinates to derive site-specific assessment parameters from a chosen meteorological database, such as the National Solar Radiation Database of NREL, Meteonorm, Explorador Solar, and NASA-SSE. These meteorological parameters served as input for conducting the PV system's performance metrics, utilising established equations and computational methods. For the computational modelling of the hypothetical 20-kWp grid-connected solar PV systems with different PV cell technologies, Solargis Prospect, pvPlanner, and PV*SOL software applications were exploited. The computational modelling process adhered to a comprehensive five-stage methodology, outlined in the flowchart presented in Fig 1.

The 5-stage process commences with a location description, where we leverage the latitude and longitude coordinates to access and generate meteorological parameters for the specified location in the second stage. In the third stage, we define the configuration of the PV system, considering factors such as orientation, user requirements, and other system-related information for a hypothetical 20-kWp grid-connected PV system.

This study considered PV cell technology, installed capacity and method of installation, and panel's orientation based on optimisation conditions in the solar PV potential and system evaluation. This input information is used to compute the meteorological and performance parameters of the solar PV system. Some of these parameters are daily, monthly, and yearly irradiation levels, energy production, annual yield, and system losses, the study will use the PV*SOL, PYsyst, and Solargis software applications based on input optimisation considerations. Additionally, a tabular comparative analysis overview of critical PV system parameters was provided. Generally, a grid-connected PV system comprises solar PV panel arrays, solar inverters, electrical panels, panel mounting racks, cables, meters, combiner boxes, surge protection, disconnects (array DC disconnect, inverter DC disconnect, inverter AC disconnect, exterior AC disconnect), grounding equipment, and other electrical accessories.

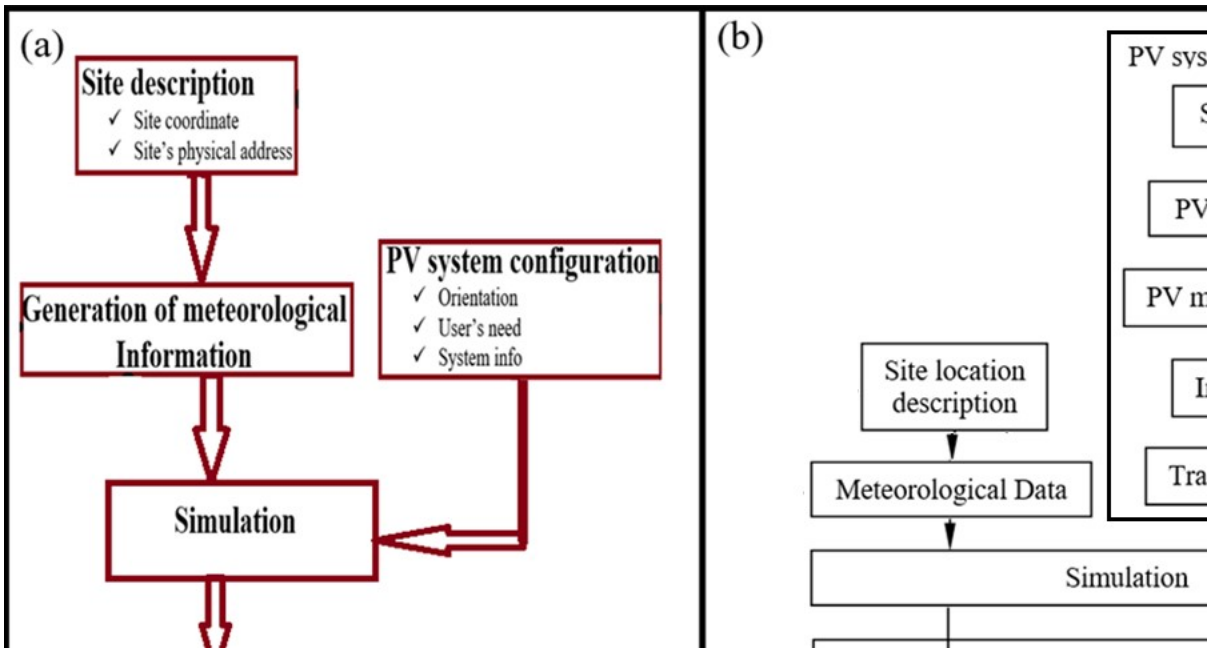

Fig. 1: PV assessment and system performance evaluation 5-stage procedure (a) the procedure block diagram; (b) the procedure flowchart.

This entails specifying parameters, such as the choice of PV cell type, installed capacity, and the energy needs of the user. The data generated in the second stage, combined with the system information defined in the third stage, serve as essential inputs for conducting simulations in the fourth stage. These simulations are carried out using PV assessment and design software applications. An additional iteration is introduced in the third stage to accommodate the application of three different PV cell technologies. The final step of this 5-stage process involves generating a report and subsequently extracting technical information from the simulation reports obtained through these software applications. This information is then utilised to analyse and assess the level of solar PV utilisation and predict the performance of the system. Other commonly employed PV system design, simulation, and analysis software applications include [17-19]:

PVSOL proves invaluable for conducting the planning and modelling of a PV system, considering factors like energy consumption, grid feed-in, and the estimation of CO_2 emissions reduction. The key input parameters for PVSOL encompass location details, meteorological data, and information related to the system and its auxiliary components.

PVGIS specializes in conducting PV system assessments based on geographical regions and offers policy support for the European Union. It requires input parameters such as total irradiance, mounting position, and monthly ambient condition values.

PVsyst, much like Solargis, serves as a tool for designing and simulating PV systems. Its capabilities encompass economic and technical assessments, system sizing, and comprehensive analysis of PV systems. PVsyst categorizes PV systems into various types, including pumping, stand-alone, grid-connected, and DC-grid systems. The necessary input variables include site location details, Albedo specification, PV panel orientation, and system sizing parameters.

Solargis Prospect, on the other hand, is an online-supported software application designed for PV system design, simulation, and analysis. It offers satellite-based mapping, technical and economic feasibility assessments, as well as planning and optimization capabilities. This tool also facilitates a comparative analysis of energy generation performance across different PV cell technologies. It relies on input parameters such as site coordinates, PV cell technology type, AC/DC losses, cable sizing, and load demand. Solargis Prospect employs a sophisticated multi-source overlay analysis approach to establish a solid foundation for a more accurate evaluation of practical PV potential. In cases where multiple layers of input parameters originate from various sources, this application integrates and harmonizes them, ensuring a cohesive and comprehensive assessment [36]. The Solargis database, from which it draws its data, is derived from multiple numerical weather models, and Table 1 provides a summary of these models.

Table 1. Summary of models deployed in Solargis [37].

Data Source	Original spatial resolution (°)	Original time resolution (hour)
European Environment Agency (ERA5), and the fifth generation European Centre for Medium-Range Weather Forecasts (ECMWF) atmospheric reanalysis of the global climate	0.25 by 0.25	1 hour
Climate Forecast System (CFSv2)	0.205 by ~0.205	1
Global Forecast System (GFSprod)	0.12 by ~0.12	1 (first 72h) 3 (up to D+9)
Global Precipitation Climatology (GPCC) version 2018	0. 25 by ~0.25	Monthly means

For this particular study, we selected two computational modelling applications, PVsyst, PV*SOL and Solargis Prospect, from the array of available PV system design and simulation tools. These choices were made due to their high accuracy, user-friendly interfaces, simplicity, widespread availability, and the clarity of the reports they produce.

3.1. Meteorological parameters

A precise and in-depth knowledge of solar radiation is important in the fields of solar energy, biomass, agriculture, human health, and climate. The deployment of satellite images is presently a vital means for the estimation of irradiance. Global irradiation is created by the three components formed by the irradiance that descended from the sun to the earth's surface. A portion is unaltered (direct normal irradiance, DNI), another portion is reflected (reflected irradiance (RHI), and the third part is dispersed by the atmosphere (diffuse horizontal irradiance, DHI). This occurrence accounts for the three components of insolation that defined the global irradiation, as shown in Fig 2(a). The GHI reaches about 1000 W/m2 in cloudless and clear weather and is measured with a pyranometer or solarimeter, shown in Fig 2(b).

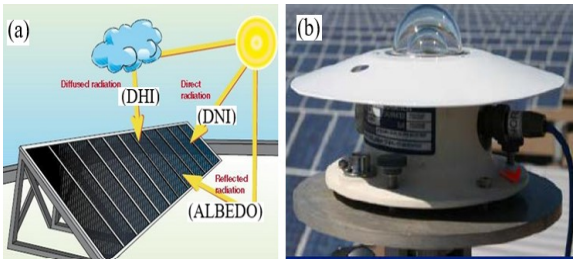

Fig. 2: (a) The components of GHI: (b) Pyranometer to measure GHI on the ground (GHI).

A part of the irradiance that is emitted to the earth is reflected and the amount of reflection depends on the reflection coefficient of the surface, called albedo. Albedo is the ratio of the reflected irradiance to the incident irradiance. The value of albedo ranges from 0 to 1 and is a dimensionless quantity. Perfectly reflecting and absorbing surfaces have an albedo of 1 and 0, respectively [38, 39]. The albedo is taken as greater than 0.8 and less than 0.03 if the surface is perceived as white and black, respectively.

3.1.1. Mathematical calculation of insolation

The insolation analysis tools compute irradiation throughout a landscape or for a specific location and this is centred in the hemispherical view-shed algorithm methods established by Rich et al. [40, 41]. The estimation of total radiation, known as global radiation, depends on location. The computation of global diffuse and direct radiations is repeated for every location on the topographic surface, creating total geographical area irradiation maps.

Global radiation calculation - The theoretical PV potential is defined by the longstanding energy content of the solar PV resource obtainable at a certain place. A plane of array irradiance (POA) is used to measure the incident irradiance on a specific PV array. The parameter is directly related to the PV module power output and is used widely in PV array modelling and performance analysis. The physical parameter GHI or POA irradiance quantifies energy content appropriately and is estimated by the summation of DNI and DHI incidents on a surface with a specified angle of incidence (AOI) and tilt. The POA is expressed as [42]:

$$Global_{tot} = GDir + GDif + GRf \quad \text{(1)}$$

Where *GDir, GDif, and GRf* are direct, diffuse, and reflected irradiations, respectively.

Considering the total irradiance received by a horizontal surface at ground level on a clear day, as represented in Fig 3:

$$Global_{tot} = G_{Dir} + G_{Dif} \quad \text{(2)}$$

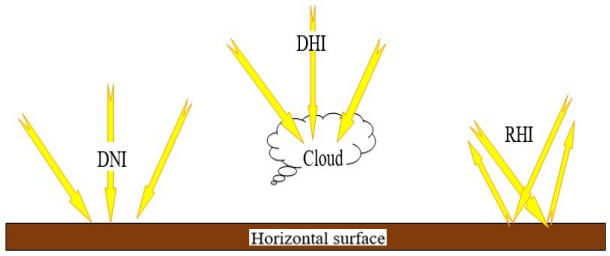

Fig. 3: Irradiance on a horizontal body

To compute the irradiance components on a tilted surface, the GHI needs to be separated into DNI and DHI. Empirical relations have been developed to calculate DHI in terms of GHI and solar zenith angle (θ_z) [43, 44]:

$$Global_{tot} = G_{Dif} + G_{Dir} * \cos(\theta_z) \quad \text{(3)}$$

$$G_{Dif} = DHI * \frac{1+\cos(tilt)}{2} \quad \text{(4)}$$

$$G_{Rf} = Global_{tot} * Albedo * \frac{1-\cos(tilt)}{2} \quad \text{(5)}$$

$$GDir_{tot} = \Sigma GDir_{\theta,\alpha} \quad \text{(6)}$$

$$GDir_{\theta,\alpha} = S_{Const} * \beta^{m(\theta)} * SunDur_{\theta,\alpha} * SunGap_{\theta,\alpha} * \cos(AngIn_{\theta,\alpha}) \quad \text{(7)}$$

Where $G_{Dir\theta,\alpha}$ is the direct radiation from the sun map sector $(G_{Dir\theta,\alpha})$ with a centroid at zenith angle (θ) and azimuth angle (α); β is the transmissivity of the atmosphere; S_{Const} is the solar constant, and 1367 W/m^2 is usually used in the analysis; $SunDur_{\theta,\alpha}$ is the time duration depicted by the sky sector; $m(\theta)$ is the relative optical path length; $SunGap\theta,\alpha$ is the gap fraction for the sun map sector; $AngIn_{\theta,\alpha}$ is the angle of incidence

between the axis normal to the surface and centroid of the sky sector.

Relative optical length, $m(\theta)$, is a function of solar zenith angle (θ) and elevation above sea level. For zenith angles less than 80°, relative optical length, $m(\theta)$:

$$m(\theta) = EXP\left(-0.000118 * Elev - 1.638 * 10^{-9} * Elev^2\right) / cos(\theta) \quad (8)$$

The angle of incidence ($AngInSky_{\theta,\alpha}$):

$$AngIn_{\theta,\alpha} = acos\left(Cos(\theta) * Cos(G_z) + Sin(\theta) * Sin(G_z) * Cos(\alpha - G_a)\right) \quad (9)$$

Where G_a is the surface azimuth angle and G_z is the surface zenith angle

A precise estimate of solar PV system radiation energises is a prequel to PV system performance evaluation, as this ensures an accurate prediction of the amount of PV energy to be generated across the year. The process of solar radiation estimation of a given location is complicated and characterised by variability and uncertainty. This has spurred studies over the years leading to the development of software applications, such as Solargis Prospect, PVsyst, Homer, and Meteonorm that simplify the process [45-48]. This study exploits the application of Solargis PV*SOL PV design application to generate the solar insolation parameters and study the performance of PV systems in winter and summer seasons.

3.2. Azimuth angle (α) and tilt angle (β)

The maximal conversion performance efficiency (CPE) of commercial poly/mono c-Si PV panels is about 24% [49], far away from 100%. In addition, other variables could affect even the 24% CPE if not properly resolved during the design and installation process. One such variable that influences CPE highly is PV panel orientation, defined by the Azimuth (α) and tilt (β) angles. This is because an inclined angle changes the solar radiation reaching the surface of the panel. Keeping this inclination relationship between the PV panel and the sun produces the maximum daily energy, and this is achieved using a mechanical tracking system. Normally, the Hemisphere determines the optimal tilt and azimuth angles; the North and South Hemispheres require southward and northward orientations for optimization, respectively [50]. The performance of solar panels is negatively impacted if the panel is wrongly orientated. It implies that for countries like Canada, China, India, and America PV panels reach optimal when they are placed in the south while the reverse is the case for countries like Brazil, New Zealand, Indonesia, South Africa, Australia, and Zambia. Subsequently, PV module spatial configuration is normally considered for maximising daily, monthly, and annual energy performance.

Several theoretical and empirical studies have established links among these parameters - the panel's Azimuth and tilt, location, period, and duration, and the impact of tilt angle on the PV panel's PCE have been reported. Maximum energy is harvested when solar irradiation strikes on PV panels placed in an optimum inclination, defined by tilt and Azimuth angles. The optimal PV panel orientation is influenced by the period and season, such that the optimum tilt angles for summer, autumn, spring, and winter vary [51]. In this context, a very clear distinction between optimal tilts for summer and winter has been reported. For many of the studies, the evaluation of the optimal tilt for the site where PV panels are facing the equator requires two variables, the location's latitude *(ϕ) and* the Hemisphere. Solar panels perform best when they are facing the equator, which implies that for a site located in the Northern Hemisphere, solar panels should face the south, as presented in Fig 4, otherwise, they should face the north [52].

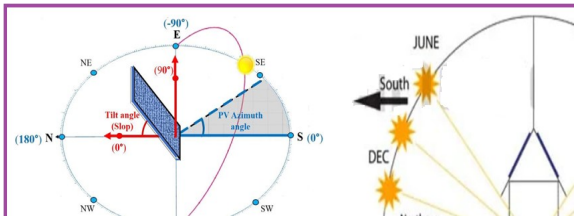

Fig. 4: Schematic of the orientation of solar panels located in the Northern Hemisphere [52, 53].

However, there exist differences in the suggested expressions to estimate optimal tilt (β), as presented in the following relations:

$\beta = \phi + 10$ [54]; $\beta = \phi - 10$ [55];

$\beta = \phi + 20$ [56];

$\beta = \phi + (0 \rightarrow 30)$ [57];

$\beta = \phi + (10 \rightarrow 20) + 10$ [58];

and $\phi + (10 + 30)$ [59],

where the latitude, ϕ, is in degree (°).

Influence of seasonal variations - Seasonal variations have a significant influence on the performance of solar PV systems. Solar PV systems generate electricity by converting sunlight into electrical energy using solar panels. The amount of energy produced by a solar PV system can vary throughout the year due to several factors related to seasonal changes. Overall, while seasonal variations do impact the performance of solar PV systems, proper planning, design, and maintenance can help mitigate these effects and ensure a reliable source of clean energy throughout

the year. To maximise the performance of a solar PV system throughout the year, it's important to consider these seasonal variations when designing and installing the system. Some strategies to mitigate the impact of seasonal variations are presented in Table 2.

Table 2. Strategies to mitigate the impact of seasonal variations.

Tilt and Orientation	Adjusting the tilt and orientation of solar panels to optimize their angle relative to the sun's path can help improve energy production throughout the year
Seasonal adjustments	Some solar PV systems have adjustable mounts that allow for seasonal adjustments, so panels can be tilted differently in the summer and winter to capture more sunlight
Energy storage	Using energy storage solutions such as batteries can help store excess energy generated during sunny seasons for use during periods of reduced sunlight
Maintenance	Regular maintenance, including cleaning and snow removal (if applicable), can ensure that the panels operate at their peak efficiency.

The positioning of a solar panel has a direct impact on the power output of a PV system. To enhance energy production per unit area, it is essential to optimise the alignment of the solar array. Ideally, the solar panels are installed on motorised trackers, with either two axes or a single axis. This results in an increased energy production of 40% and 20%, respectively, compared to fixed PV systems [60]. However, it should be noted that this approach does come with additional operation and maintenance costs. For fixed PV systems, the most favourable orientation is typically achieved by selecting a tilt angle that is close to the latitude of the installation site and an azimuth angle that faces North in the Southern Hemisphere or South in the Northern Hemisphere. To optimise energy production throughout the year, a common rule of thumb is to set the tilt angle roughly equal to the latitude of your location. This means the tilt angle would be approximately equal to the latitude. In this study, the optimal tilt angle (β_{opt}) for all year-round energy production is taken as the latitude (ϕ).

Tilt angle (β_{opt}) = latitude (ϕ) = *30*

In the northern hemisphere, a south-facing orientation is generally optimal for year-round energy production. In the southern hemisphere, a north-facing orientation is typically ideal. It implies that the Azimuth angle *(α)* is 180° for a south-facing system and α is 0° for a north-facing orientation [61, 62]. To optimise energy production for a specific season (winter or summer), more complex calculations or software tools take into account solar angles and seasonal variations. The goal is to adjust the tilt angle to capture more sunlight during that season. The influence of seasons (summer and winter) on PV performance was considered quantitatively and qualitatively in estimating the optimum tilt angle as follows [63]: $\beta = \phi \pm 20$ and $\beta = \phi \pm 8$, where + and – were applied for winter and summer, respectively. However, the expressions to estimate season-based tilt were grouped into two methods [53].

i. Method 1: $\beta = \phi \pm 15$ again, where + and – were applied for winter and summer, respectively.

ii. Method 2: $\beta = 0.9\phi + 29$ for winter, $\beta = 0.9\phi - 23.5$ for summer and this method was referred to as an improvement of method 1 with better results.

Apart from solar panel orientation, other factors, such as panel quality, inverter efficiency, and system maintenance are other aspects of designing an efficient PV system that contribute to overall performance.

3.3. Photovoltaic system performance

Solar PV potential refers to the amount of solar energy that can be harnessed in a specific geographic area and this depends on the magnitude of the sun's radiation reaching the panel. This potential is influenced by various factors, including the location, PV panel orientation, seasons, climate, available technology, and the specific characteristics of the solar PV system. Analysing the performance of a PV system is essential to assess its efficiency and productivity. It is also crucial for optimising energy production, maintaining the long-term sustainability of the system, and ensuring a good return on your investment. According to IEC standards 61724-1 [64], some of the key steps and metrics involved in analysing the performance of a PV system include [65]:

3.3.1. Electricity production and specific yield calculation

The electricity production of a PV system is the total amount of electrical energy generated by the system over a given period. This electricity production is typically in kWh and can vary depending on certain factors, such as the system's capacity, the amount of sunlight reaching the panel, and its efficiency.

The specific yield of a PV system is a metric used to evaluate the system's performance and efficiency. Specific yield is the amount of electricity produced by the PV system per unit of its installed capacity, typically measured in kWh per kilowatt-peak (kWh/kWp). The kilowatt-peak (kWp) is a measure of the system's maximum power output under standard test conditions (STC). This metric helps compare the performance of different PV systems and is mathematically expressed as:

$$Specific\ yield = \frac{Total\ energy\ production\ (kWh)}{Installed\ capacity\ (kWp)} \quad (15)$$

3.3.2. Performance ratio

Performance ratio, also known as a quality factor, measures the quality of a PV system by accounting for the system's losses, such as soiling losses, mismatch and wiring losses; light-induced degradation (LID); system downtime, inverter and transformer losses, and many more [66, 67]. Additionally, PR takes into account irradiation, relative humidity (RH), temperature, and climate changes. It uses a vague correction factor in % to make up the difference between the expected (theoretical) power output rating and the actual performance [68]. A typical PR value is between 50% and 60% for a stand-alone PV direct current (DC) power-

delivering system and 70% and 80% for a grid-connected alternating current (AC) delivering system [69]. Again, PR can be defined as the ratio between the standard electricity production (Y_f) and the available solar potential (Y_r), expressed as:

$$PR = \frac{Y_f}{Y_r} \quad (2)$$

$$= \left(\frac{E_{PV}}{P_{norm} A} \right) Y_r \quad (3)$$

The performance ratio was expressed according to the IEC-61724-1 standard by a study [70], as in equation (4):

$$PR = \frac{\left(\sum_k P_{out,k} * \tau_k \right)}{\left(\left(\sum_k P_o * G_{i,k} * \tau_k \right) / G_{i,ref} \right)} \quad (4)$$

Where τ_k is the period; $G_{i,ref}$ is the POA during reference conditions; P_o is the power out under reference conditions; and $G_{i,k}$ is the in-plane irradiance (POA) at period k.

4. COMPUTATIONAL MODELLING OF A 20-KWP GRID-CONNECTED PV SYSTEM

This section comprehensively covers all technical aspects of the PV system, ranging from the assessment of its potential to the evaluation of the proposed installed system's capacity performance. This includes configuring the PV system, and conducting simulations for the three selected PV cell types and at different tilt angles (β_{opt}, β_{win}, and β_{sum}). The reports of these scenarios were used for analysing, comparing, and establishing the solar PV potential using insolation and the system's performance in terms of energy generation, losses, and the reduction of CO_2 emissions.

4.1. Site location description and system configuration

A fundamental step is describing the PV system's site, which can be done through latitude and longitude coordinates, a coordinate system, or a physical address. For this study, we hypothetically positioned the 20 kWp-installed capacity PV system in Mountain Rise, Durban, South Africa, with latitude/longitude coordinates of 29° 52' 50.7" S, 30° 58' 12.3" E (coordinates -29.88075°,030.970083°). The configuration details of the PV system include design considerations like system capacity, user power requirements, PV cell selection, and panel orientation. In this study, a computational modelling optimisation tool was exploited to obtain the tilt angles for all year-round (β_{opt}), winter (β_{win}), and summer (β_{sum}) seasons. Table 3 presents the site information and the PV system's configuration.

Table 3. Site's description and system configuration information

Site location description						
Site location (Lat/Lon)	-29.88075°,030.970083°				Physical address	Mountain Rise, Durban, South Africa
PV system type	Grid-connected					
User's need	Household	Night ratio (%)			49.6	
Average power (W)	139	Daily energy			3.3 kWh/day	
PV Field Orientation						
Fixed plane	Azimuth 0°	β_{opt} 30°	β_{win} 10°	β_{sum} 48°	Installation type	Roof mount
Nb. of modules	7 units				Pnom total	2100 kWp
PV cell type (%)	c-Si (mono)	CdTe			CIS	

5. RESULTS AND ANALYSIS

Primarily, there are four types of seasons in Durban, South Africa, as follows [71]: Summer – (November-March); Autumn – (April-May); Winter – (June-August); and Spring – (September-October). The summary of Durban's weather conditions across the year is - the rainy season from late November to January, while it is clear and windy most of the year, with the yearly temperature varying between 14 °C and 28 °C. However, in this study, the seasons are categorised into two: Winter – (April to September) and summer – (October to March). The present versions of Solargis and PVsyst have no discrete information linking autumn and spring seasons to PV meteorological parameters. This study is confronted with meteorological data limitations for the autumn and spring seasons in the software applications used. For optimisation, the design and simulation process maintained the same Azimuth (north, 0°), 30°, 10°, and 48° were used for tilts β_{opt}, β_{win}, and β_{sum}, respectively. and fixed surfaces were considered for the two seasons' PV panels' configuration.

5.1. Solar PV assessment

In this section, the impacts of PV panel orientation and seasons were exploited to analyse PV potential and expected energy output of a solar PV system to determine the feasibility of the energy system. This information is crucial for making informed decisions about solar PV installations and their economic and environmental benefits. The GHI and GTI are the most relevant insulation components in the context of electricity production from solar energy.

5.1.1. Site location insolation

The monthly profile of temperature and components of insolation that contribute to the PV potential expected to produce electricity are in Fig 5(a). It is evident from Fig 5 that:

i. The three radiation components presented in Fig 5(a) exhibit the same profile patterns. The highest monthly average irradiance (174.7

kWh/m²) was recorded in January, while the lowest (94.4 kWh/m²) was observed in June.

ii. The yearly sum of GHI, DNI, and DIF, as shown in Fig 5(b) are 1630.5 kWh/m², 1566 kWh/m², and 642 kWh/m², respectively.

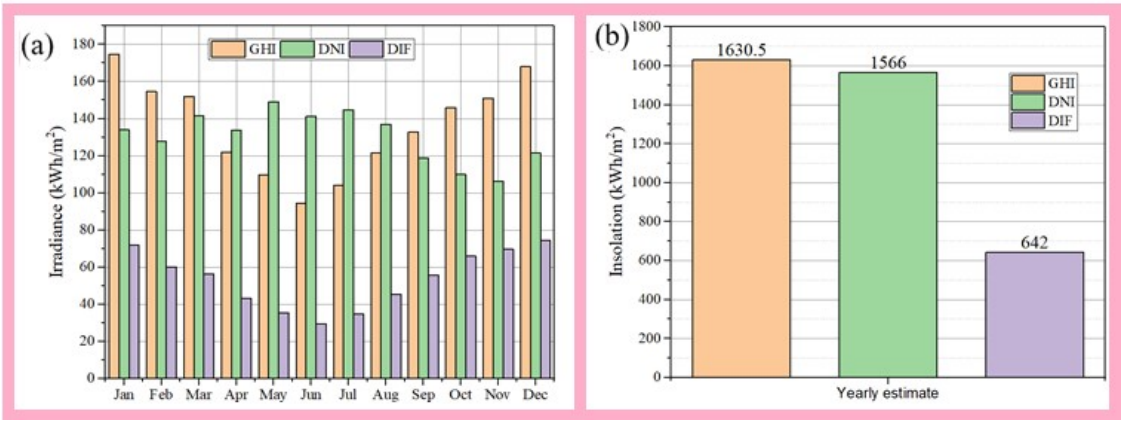

Fig. 5. Solar insolation components (a) the monthly average of GHI, DNI, and DIF; (b) the monthly sum of global irradiation and daily (diurnal) air temperature.

5.1.2. Solar panel orientation and season-based PV potential assessment

The earth is continuously in motion, moving across the sky and this affects the radiation that gets to the solar PV panels. A tracking device was developed to augment this movement and to ensure that the PV panel or collector aligns with the sun at a defined angle automatically. This is to maintain the optimum angle required to harvest and convert most of the solar irradiation. However, this in most cases is not possible for rooftop-mounted PV panels. The PV panel is orientated in a defined manner to optimise the PV panel's conversion performance. This is achieved by tilting the panel to face the sun, and studies have proved that this method produces more energy [72-74].

Global in-plane irradiation, also recognized as global tilted irradiation (GTI), global tilted solar radiation, or global plane-of-array irradiance, represents the total solar irradiance reaching a solar PV panel or collector inclined at a specific angle and oriented in a direction. This factor plays a pivotal role in the design and evaluation of solar energy systems as it considers the actual solar energy incident on the panels, accounting for their tilt and orientation. Global tilted irradiation offers a more precise measure of the energy available for electricity generation compared to GHI. This affirmation is further substantiated by the results derived from the simulation report presented in Fig 6. The outcomes in Fig 6(a) can be summarised as follows:

i. The annual cumulative irradiance of GHI (Gh_m, 1636 kWh/m^2) reaching the panel remains consistent for all year-round and season-based tilt concepts.
ii. The annual cumulative irradiance of GTI (Gi_m) reaching the panel differs across various tilt concepts, both for year-round and season-based configurations (10° = 1839.3 kWh/m^2, 10°/48° = 1921 kWh/m^2); Gi_m<Gh_m.
iii. The percentage increase in irradiance reaching the panel when transitioning from Gh_m to Gi_m, that is, from β_{opt} (30°) to β_{win}/β_{sum} (10°/48°) is approximately 12% and 15%, respectively.

In Fig 6(b), it is apparent that:

i. The annual cumulative irradiance losses are more pronounced at β_{opt} = 30°.
ii. In the scenarios of βopt = 30° and βwin/βsum = 10°/48°, the most substantial irradiance losses occur in the summer and winter, respectively.

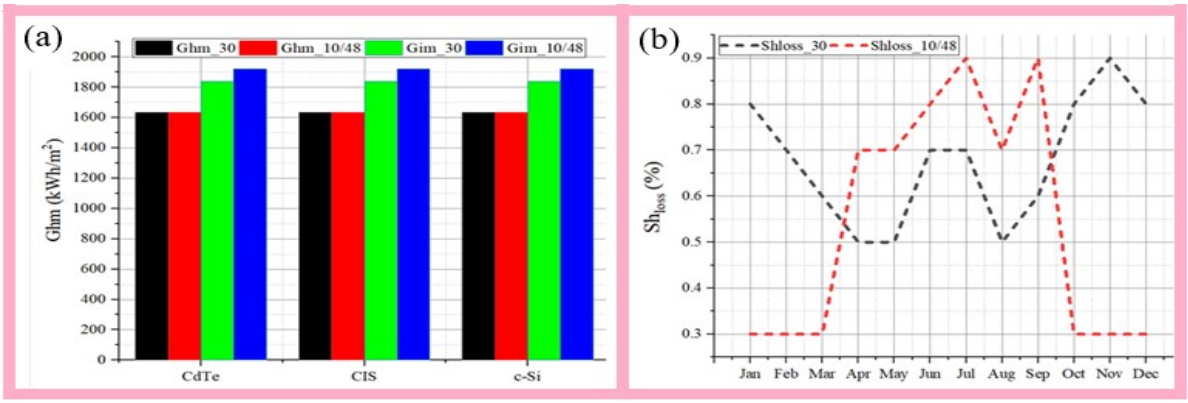

Fig. 6: Impact of PV panel tilt on PV potential (a) the yearly sum of irradiance reaching the panel; (b) the profile of yearly irradiance loss per orientation.

Where Gh_m is a profile of the monthly global horizontal irradiation (GHI, kWh/m^2) in a year, Gi_m is the monthly sum of global tilted irradiation (GTI, kWh/m^2), and Sh_{loss} is the losses of global irradiation by terrain shading (%).

5.2. Photovoltaic potential in winter and summer

Data extracted from the study's report reveals that the PV potential and profile exhibit seasonal variations. In Fig 7, the following observations can be made:

i. The site's irradiance levels reached their highest and lowest points in May (166.4 kWh/m^2) and September (148.5 kWh/m^2) during the winter season, while in summer, the highest and lowest irradiance levels occurred in January (173.9 kWh/m^2) and October (149.3 kWh/m^2) respectively (as depicted in Fig 7(a)).
ii. Winter saw the highest and lowest ambient temperatures in April (21.5 °C) and July (17.5 °C) respectively, while in the summer season, the highest and lowest ambient temperatures were observed in February (23.9 °C) and October (20.4 °C) respectively (as shown in Fig 7(b)).

In Fig7(c)&(d), the following observations can be made:

iii. The total sum of GTI and losses displayed variations concerning tilt angles and seasons. Notably, the all-year-round tilt angle of 30° recorded the lowest values.
iv. During winter (refer to Fig 7(c)), the total sum of GTI (957.8 kWh/m2) and losses (4.7%) observed at a 10° tilt angle were higher than what was produced at a 30° tilt angle (GTI, 920 kWh/m2 and loss, 3.5%). Similarly, a total sum of 963 kWh/m2 and losses of 1.8% was recorded at a 48° tilt angle, while a 30° tilt angle produced GTI of 920 kWh/m2 and losses of 4.6% (as seen in Fig 7(d)).
v.

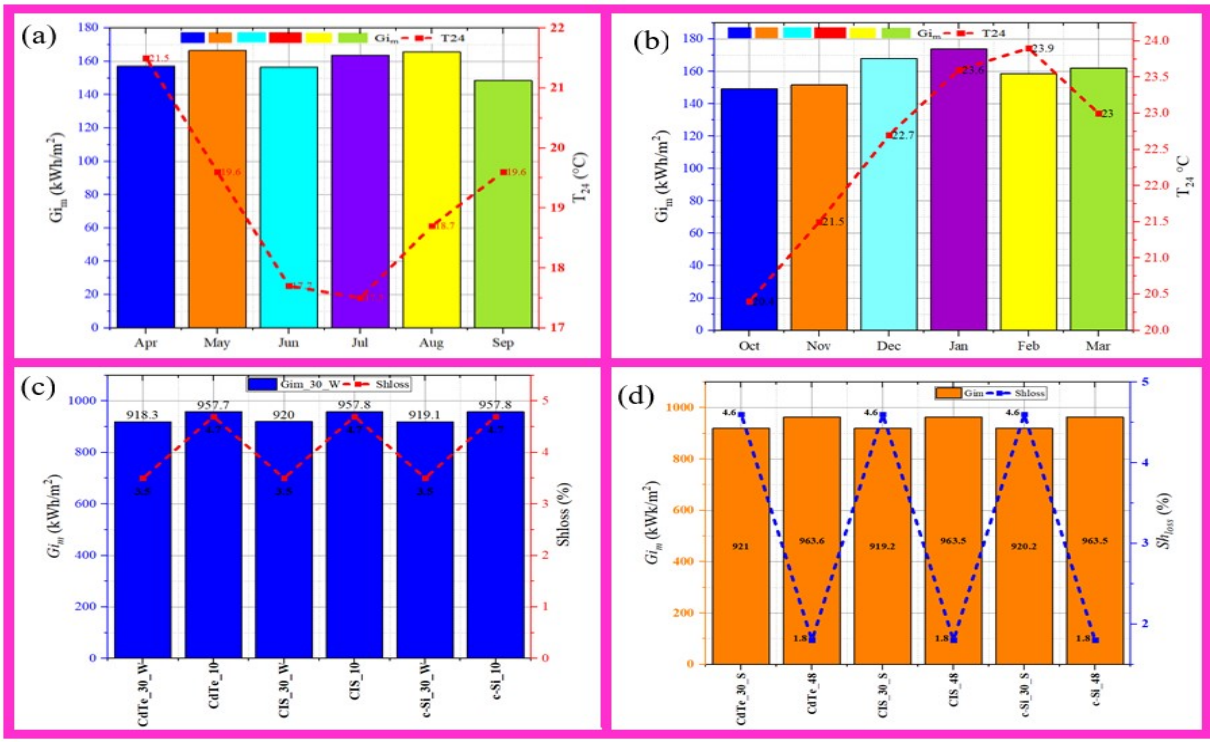

Fig. 7: Season-based PV potential (a) a profile of GTI and temperature during winter; (b) a profile of GTI and temperature during summer; (c) the total sum of GTI and loss at different tilt angles during winter; (d) the total sum of GTI and loss at different tilt angles during winter.

Where Gi_m is the monthly sum of global irradiation (kWh/m^2); T_{24} is the daily (diurnal) air temperature and Sh_{loss} is the terrain shading (%).

5.3. The performance of the 20-kWp PV system

The performance of the PV systems of 20 kWp-installed capacity of the three selected PV cells based on the year-round and two-season (winter and summer) tilts. The performances of the PV cells were summed up in this section. The performance evaluation was based on the following parameters - specific electricity production, total electricity production, PR, own consumption and grid feed-in, and reduction of CO_2 emissions.

5.3.1. Photovoltaic electricity production

Based on the data obtained from the study's report, it is observed in Fig 8 that:

i. At β_{opt} and β_{win}/β_{sum}, the c-Si PV system produced the least energy, 1414 kWh/kWp and 1503 kWh/kWp, respectively, while the CdTe PV system generated the highest energy at β_{opt} and $\beta_{win}/\beta_{sum,}$ 1522 kWh/kWp and 1609 kWh/kWp, respectively.
ii. The highest and lowest PR was observed in CdTe (83.3%) at β_{win}/β_{sum} and c-Si (76.4%) at β_{opt}.

According to Fig 8, the relationship between irradiance and PV energy generation is direct

proportionality. There is a direct and linear relationship between irradiance and PV energy generation. When the irradiance on a solar panel increases, the energy output of the panel also increases.

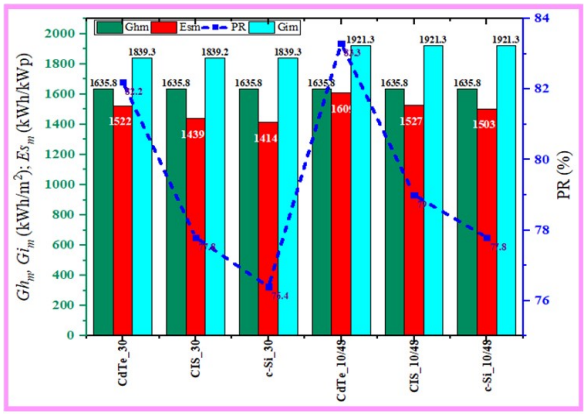

Fig. 8: Energy conversion steps and losses (a) energy output of the various PV cells; (b) yearly sum of Global in-plane irradiation (kWh/m²).

Further, the production of energy by the PV system does not follow only the irradiance magnitude trend, Figs 9 and 11 show that the type of PV cell technology and tilt angle deployed play a significant role. Higher specific electricity production is achieved through the deployment of high PCE PV cells and season-based optimal tilts. Fig 9 reveals that:

i. In Fig 9(a), the CdTe PV system produced the highest PV specific electricity in both seasons at β_{opt} and β_{win}/β_{sum} and the lowest PV specific electricity generation was observed in the c-Si PV system at both seasons.

ii. In Fig 9(b), the CdTe PV system produced the highest PV-specific electricity in the summer season at β_{opt} and β_{win}/β_{sum} and the lowest PV-specific electricity generation was observed in the c-Si PV system at both seasons and scenarios.

As observed in Fig 9, the season-based tilt system generated more electricity than all year-round tilt systems, hence, the electricity generation discussion will be based on a season-based approach.

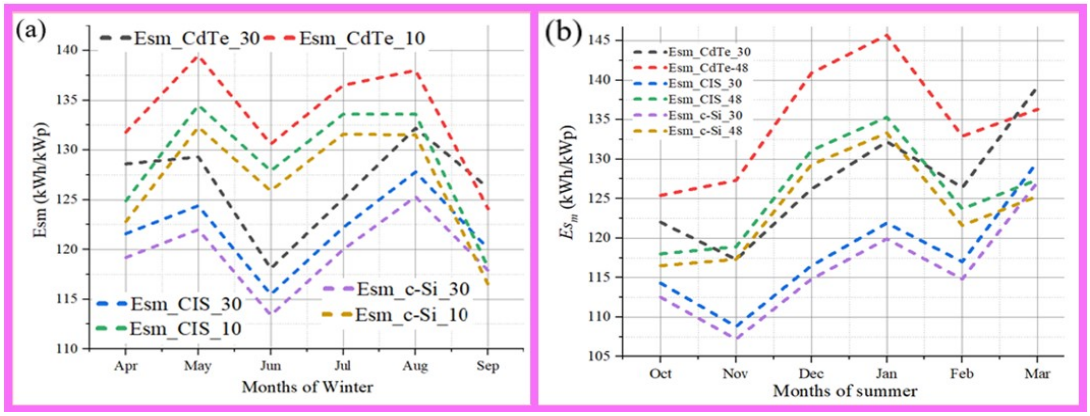

Fig, 9: The profile of specific electricity production by PV systems at varied tilts (a) in the winter season; and (b) in the summer season.

The study further in Fig 10 reveals that:

i. The β_{win}/β_{sum} tilt concept generated greater specific electricity than the β_{opt} approach of all the PV cells (see Fig 10(a)).

ii. There is a rise in the yearly specific electricity generation in transitioning from β_{opt} and β_{win}/β_{sum} tilts, as depicted in Fig 10(b). The percentage increase in the sum of the yearly specific electricity generation between the β_{opt} tilt and β_{win}/β_{sum} concept of CdTe, CIS, and c-Si PV systems was 5.66%, 6.06%, and 6.35%, respectively.

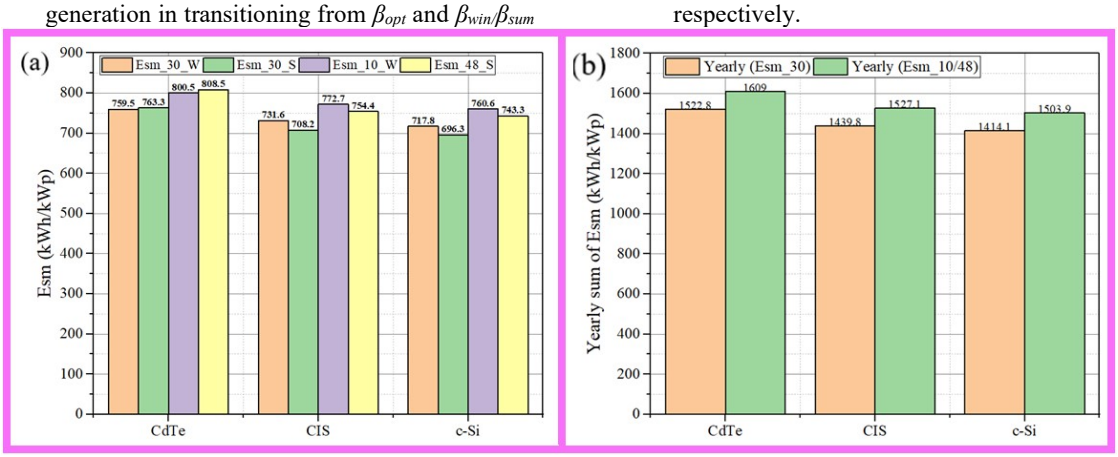

Fig. 10: Specific electricity production (kWh/kWp) (a) monthly sum; (b) yearly sum

Where Es_m is the sum of specific electricity production monthly (kWh/kWp); Es_d is the sum of specific electricity production daily (kWh/kWp); Et_m is the sum of total electricity production monthly (MWh); E_{share} is the percentual share of monthly electricity production (%); PR is performance ratio (%).

5.3.2. Total electricity production

The findings depicted in Figure 11 are as follows:

i. During winter, CdTe exhibited the highest total electricity production (2.8 MWh) in May and August, while c-Si cells produced the lowest (2.3 MWh) in September.
ii. In summer, CdTe cells generated the highest total electricity production (2.9 MWh) in January and October, with c-Si cells recording the lowest (2.3 MWh) in November.
iii. Overall, the three types of PV cells showed their best performance in May and August during winter and in January during summer in terms of monthly electricity production.
iv. Conversely, the weakest performances were observed in September during winter and in October and November during summer.

The CdTe PV cell demonstrated the most robust performance, followed by the CIS PV cell, in total monthly electricity production in both seasons. On the other hand, the c-Si PV cell exhibited the lowest performance in monthly electricity production during both seasons. Notably, the overall performance of the three PV cells was superior in summer compared to winter in terms of monthly electricity production.

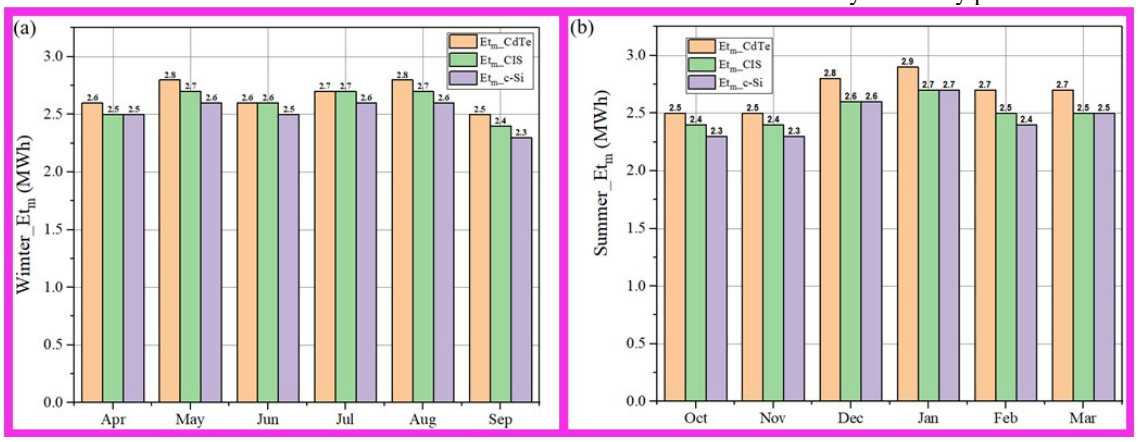

Fig. 11: The sum of total electricity production monthly in (a) the winter season; and (b) the summer season

In Fig 12, a consistent trend shows that the total annual electricity produced was lower when using the all-year-round approach across all PV cell technologies.

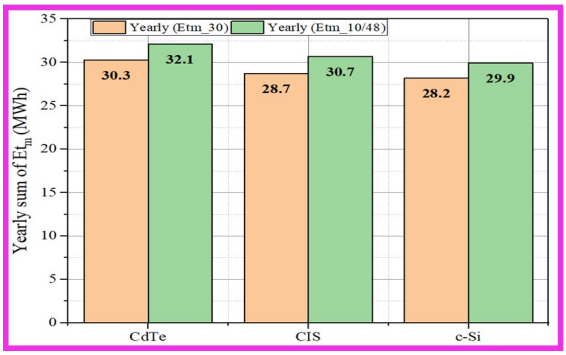

Fig. 12: The sum of total electricity production

The order of ascending performance among the three PV cell technologies remains consistent, with CdTe outperforming CIS and c-Si in both all year-round and season-based scenarios. Among the season-based tilt approaches, the highest annual electricity production was observed with CdTe (32.1 MWh), followed by CIS (30.7 MWh) and c-Si (29.9 MWh).

5.3.3. Quality of electricity generation

In this section, the PR of the three PV systems based on the selected PV cell systems as obtained from reports are presented in Figs 13 and 14 and the following observations were made:

i. In Fig 13, the average PR recorded for CdTe, CIS, and c-Si cell systems in winter are 82.9%, 80%, and 78.8%, respectively, while 83.7%, 78.1%, and 76.9% are the average PR for CdTe, CIS, and c-Si cell systems in summer, respectively. The influence of summer high temperatures on CdTe cells seems to be insignificant but it is obvious on CIS and c-Si cells, as the cells possess higher PR in winter.
ii. The result depicted in Fig 13 further portrays that the season-based tilt CdTe cell system generates electricity more than all year-round methods and other PV cell systems.

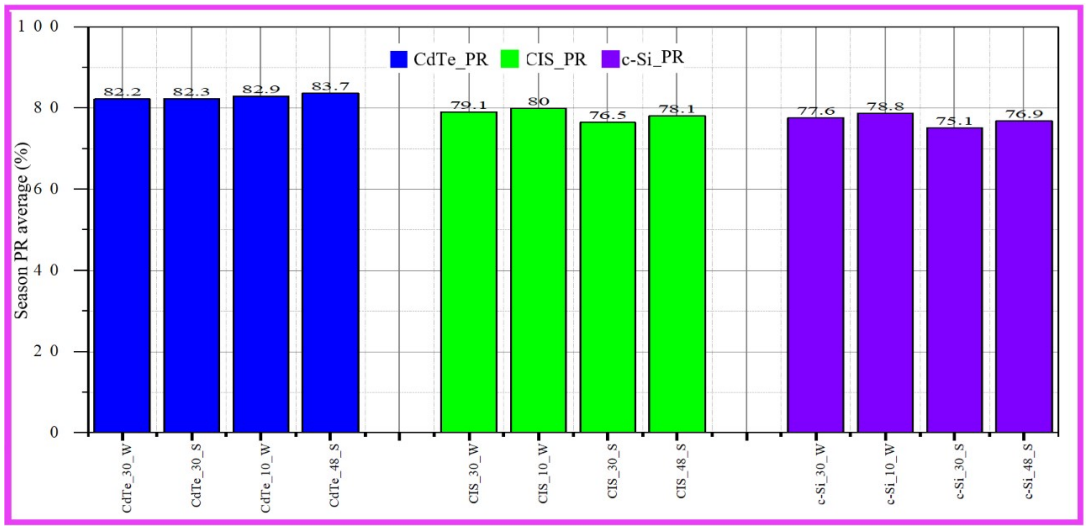

Fig. 13: Season PR average (%) of the different PV cell systems

iii. Considering Fig 14, CdTe PV cells behaved differently from CIS and c-Si cells and performed better in summer. CIS and c-Si cells were more efficient in the winter season and they have the PR profile in both seasons.

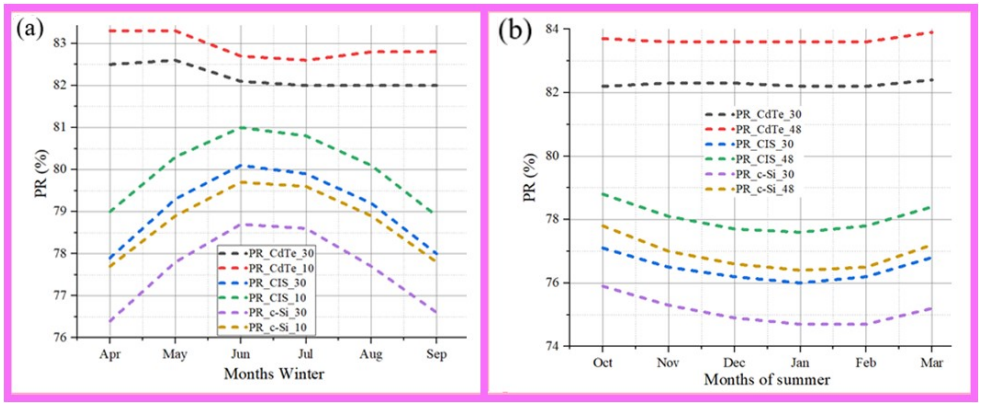

Fig. 14: The PR profiles of different PV cell systems (a) winter season; (b) summer season

The magnitude of PR depends on the various losses linked to the PV systems and this includes losses due to the electrical resistance of the wire, loss due to inverters, location of the panels, and shading. The second source of energy losses after the wire is associated with an inverter, which affects PR directly [75].

5.3.4. System losses

The findings thus far indicate that the CdTe PV system exhibited superior performance compared to both the c-Si and CIS PV systems. This performance discrepancy can be attributed to a range of system losses. Energy losses within various PV cells, including module and inverter losses of different PV cell systems, are detailed in Fig 15:

i. The highest (438 kWh/kWp) and least (323 kWh/kWp) energy losses were observed in 30° c-Si and 10/48° tilts deployed in CdTe PV systems, respectively, as shown in Fig 15(a).

ii. Fig 15(b) shows that module DC conversion, inverter DC/AC and other DC losses depend on PV cell and PV panel tilt. The lowest and highest module DC conversion losses were observed in tilt 30° c-Si and tilt 10/48° in CdTe PV systems, respectively.

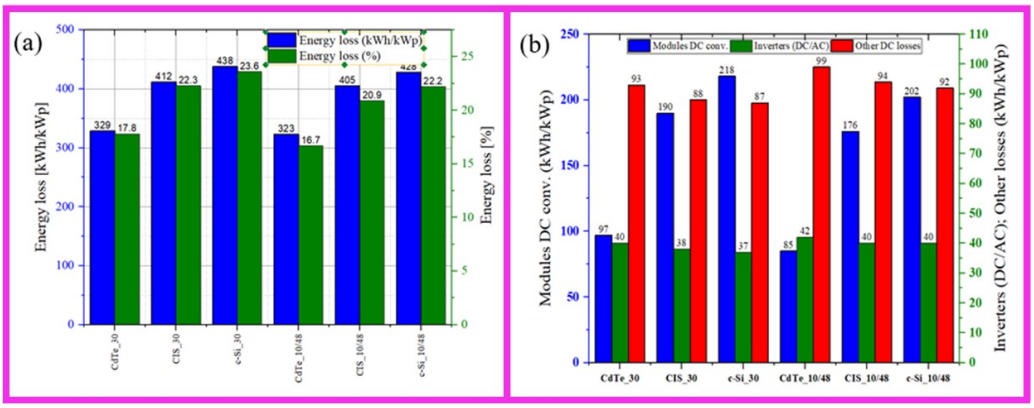

Fig. 15: Energy losses (a) energy losses by various PV cells; (b) module and inverter losses of the different PV cell systems.

These losses stem from various factors [76-78], including incident angle modifier (IAM), terrain shading, reflectivity, module quality, AC to DC conversion within the modules, as well as other elements such as inverters, DC/AC conversion transformers, AC cabling, reduced availability, soiling, light-induced degradation (LID), mismatch, module degradation, system availability, and potential-induced degradation (PID). Among these limiting factors, the primary contributors to the overall yearly loss are associated with the conversion to DC within the modules, additional DC losses, and the DC/AC conversion transformers of the inverters. The standard efficiency of inverters typically ranges between 95% and 98%, subject to the brand and quality. Inverters are tested within temperature ranges of 25 °C to 60 °C for standard inverters and 40 °C to 65 °C for micro-inverters [75, 79]. However, if inverters operate above the recommended temperature ranges, their efficiency may decline. Other sources of loss are tied to panel positioning and shading. Shading significantly impacts installation efficiency, contingent on the panel connection.

5.4. Relevant Ambient parameters that influence PV system performance

Specifically, temperature directly impacts various facets of PV systems, such as module degradation, cell and inverter efficiency, and energy and voltage output, both directly and indirectly. Elevated ambient temperatures have a noticeable impact on PV system efficiency. When a PV panel's temperature exceeds 25°C, its efficiency typically diminishes due to the temperature coefficient, which measures the degree to which output power decreases for each Celsius degree above the standard temperature, usually set at 25°C [80, 81]. The average temperature at the site in question contributes to electricity quality, being below 25°C. The highest temperature recorded (24.1°C) and the lowest (16.4°C) were observed in February and July, respectively, as shown in Fig 16(a).

Other ambient factors influencing PV system performance include wind speed (WS), relative humidity (RH), precipitable water (PWAT), and precipitation (PREC). The information derived from the study's report, as presented in Fig 16, aligns with previous comparative studies on PV potential and system assessment [82, 83]. This study indicates that the meteorological conditions in Durban, South Africa, favour the performance of PV systems.

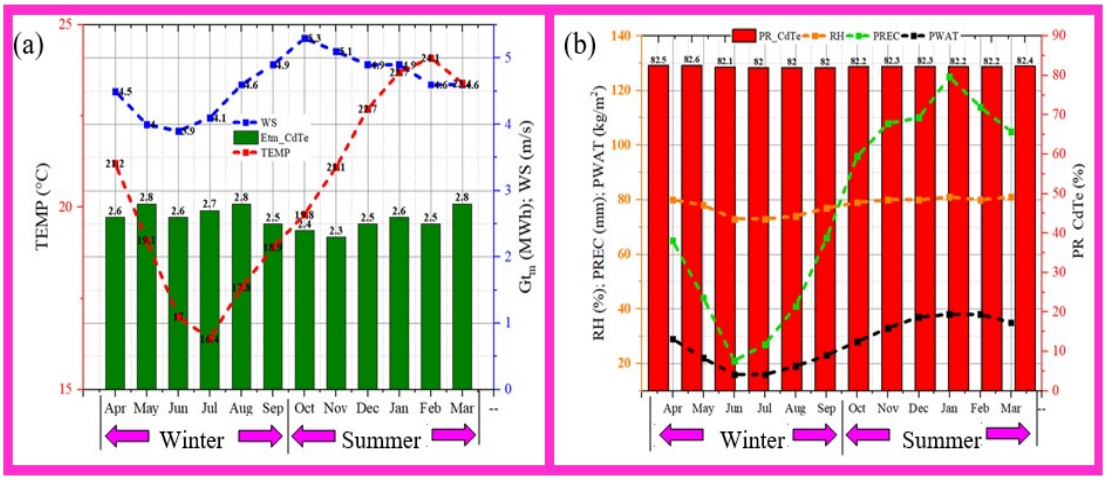

Fig. 16: Photovoltaic system ambient parameters (a) Wind speed (WS); (b) Relative humidity (RH), precipitate (PREC), and precipitable water PWAT.

Where WS is the wind speed (m/s), RH is the relative humidity (%), PWAT is the precipitable water (kg/m^2), and PREC (mm) is the precipitation (rainfall).

Elevated levels of Relative Humidity (RH) and Wind Speed (WS) have a dual impact on PV systems. On one hand, increased RH often results in heightened cloud cover and atmospheric water vapour presence. This can create clouds of humid air that scatter or absorb sunlight, subsequently reducing the solar irradiance reaching the PV panels. Additionally, excessive humidity can foster the accumulation of dirt and dust on the panel surface, decreasing efficiency due to reduced light absorption. Conversely, humidity and WS can act as a cooling mechanism for PV panels. This facilitates heat transfer through processes like evaporation and condensation, potentially mitigating some of the adverse effects of high temperatures on system efficiency.

5.5. User Consumption and Grid Feed-in

This study outlines the user's daily and annual consumptions, presented in Table 4, which were utilised to estimate the performance of PV cells concerning electrical load and the potential reduction in CO_2 emissions through PV system utilization.

Table 4. User's consumption information

Detailed User's needs					
Electrical appliances	**Quantity (*q*)**	**Capacity (W)**	**Total watts, W_{total} (W)**	**Hours per day (h)**	**Energy consumptions, $W_{h/day}$ (Wh/day)**
Compact fluorescent lamp (CFL)	2	10	130	9	180
Laptop	1	150	150	9	1350
Fan	1	75	75	9	675
Television	1	70	70	4	280
Refrigerator	1	50	50	24	1200
Washing machine	1	2	2	0.5	1
Mobile set	6	6	6	5	180
Standby consumers				24	24
Total daily energy					3,890 Wh
Total yearly energy					1,420 kWh

Considering the report obtained from the PV*SOL application, presented in Table 4, with PV panel Azimuth/tilt used as (0/30°), it was observed that the avoided CO_2 emissions in PV cell depend on PV cell, as presented in Table 5

Table 5. Own consumption and energy for grid feed-in

PV cell	c-Si	CIS	CdTe
Installed (kWp)	20.4	20.3	20.16
Annual energy (kWh)	20714	19457	19397
Own consumption (kWh)	721	707	708
Grid feed-in (kWh)	19993	18750	18689

5.6. Reduction of CO_2 emissions

Certainly, the sun stands as a vast energy source, even though our current capacity to fully harness this energy and substitute it for fossil fuels remains limited. Yet, a significant environmental impact can be achieved through the widespread installation of solar PV panels. With the adequate installation of solar panels, considerable reductions in greenhouse gas emissions, including CO_2, sulphur oxides, nitrogen oxides, and particulate matter, are attained for each kWh of solar electricity generated. The proposed grid-connected PV system in Mountain Rise, Durban, delivers the advantages of providing clean energy, saving energy, and reducing CO_2 emissions, as outlined in Table 5. Results obtained from the PV*SOL software application demonstrate that the use of c-Si cells led to the highest prevention of CO_2 emissions.

Table 5. Avoided CO_2 emissions

PV cell	Installed capacity (kWp)	Annual PV energy (kWh)	Specific annual yield (kWh/ kWp)	Avoided CO_2 (kg/year)
CdTe	20.2	19397	962.14	10,377
CIS	20.3	19457	958.48	10,409
c-Si	20.4	20714	1015.39	11,082

6. CONCLUSIONS

In this study, the investigation of PV potential at a specific location in Mountain Rise, Durban, South Africa (-29.88075° latitude and 030.970083° longitude) has been conducted. The focus was on a hypothetical 20-kWp PV system, assessing three different PV panel technologies and three tilt angles. These PV panel technologies include polycrystalline silicon, cadmium telluride, and copper indium selenide cells, and considered 30°, 10°, and 48° as optimised tilts for year-round (β_{opt}), winter (β_{win}), and summer (β_{sum}) conditions with tilt angles of maintaining a constant azimuth of 0°. To carry out this assessment, computational modelling and analysis software tools, such as Solargis Prospect, pvPlanner, and PV*SOL were employed. The study's results underscore critical meteorological parameters at the site, including:

i. Annual GHI sums up to 1636 kWh/m², while GTI measures 1839.3 kWh/m² and 1921 kWh/m² at both the year-round tilt (30°) and season-based tilts (10°/48°).
ii. Average ambient conditions for PV panels reveal TEMP, WS, and RH at 20.8°C, 4.6 m/s, and 78%, respectively.
iii. Transitioning from GHI to GTI (βopt at 30° and βwin/βsum at 10°/48°) results in percentage increases of 12% and 15%, respectively.

The assessment of PV system performance is reported as follows:

iv. Annual total electricity production (MWh) by CdTe, CIS, and c-Si PV systems at βopt amounts to 30.3, 28.7, and 28.2, respectively.
v. Annual total electricity production (MWh) by CdTe, CIS, and c-Si PV systems at βwin/βsum stands at 32.1, 30.7, and 29.9, respectively.
vi. The average performance ratio (PR) for CdTe, CIS, and c-Si cell systems in winter and summer is 82.9%, 80%, 78.8% and 83.7%, 78.1%, and 76.9%, respectively.
vii. Regardless of the PV cell type, an average of 10,623 kg/year of CO2 emissions will be avoided for a total of 1,420 kWh yearly electricity consumed.

In conclusion, the study aptly addresses climate change consequences and the role of fossil fuels in CO_2 emissions contributing to climate change. It demonstrates

substantial PV potential in Durban, highlighting increased PV energy when aligning PV panel orientation based on seasons versus the year-round approach. The study identifies the CdTe PV cell's superior performance in high-temperature conditions, positioning it as the preferred PV cell for summer season application.

7. FUTURE STUDY: RESEARCH GAPS IN PV CELL TECHNOLOGIES AND SYSTEMS

This study has identified and compiled these limitations in Table 6.

Table 6: Research gaps in PV cell technologies and systems

Long-term performance assessment	Limited studies focus on the long-term performance of PV systems in various seasons, making it difficult to ascertain their durability and reliability over time.
Seasonal efficiency variations	A need exists to investigate the extent of efficiency fluctuations across different seasons, as well as their impact on energy generation and system economics.
Climate and geographic variability	Research could delve deeper into how regional climates and geographic locations affect PV system performance, considering factors such as temperature, sunlight availability, and weather patterns.
Operational optimization	There may be gaps in optimizing PV system operations to maximize energy generation in varying seasonal conditions, particularly in off-grid or remote settings.
Energy storage integration	Exploring effective energy storage solutions and their integration into PV systems to mitigate seasonal variations in energy production and consumption.
Environmental impact	Assessing the environmental impact of PV technologies in different seasons, including the lifecycle analysis and potential ecological effects.
Technological advancements	Keeping pace with rapid technological advancements and their implications for seasonal performance, such as the development of new materials, designs, and smart-grid integration.
Economic viability	Investigating the economic feasibility of PV systems, including payback periods, return on investment, and financial incentives in different regions and seasons.
Grid integration challenges	Addressing challenges related to grid integration, especially during periods of excess energy generation or scarcity, and exploring potential solutions.
User behaviour and energy demand	Studying how user behaviour and energy demand patterns change with seasons and how PV systems can adapt to meet these evolving needs.
Policy and regulatory frameworks	Analysing the impact of policy and regulatory frameworks on the adoption and performance of PV technologies across seasons.
Data collection and analysis	Developing standardized methodologies for data collection and analysis to facilitate meaningful comparisons between studies and regions.

Addressing these research gaps will contribute to a more comprehensive understanding of PV cell technologies and systems, enabling better-informed decisions for sustainable energy solutions.

CONFLICT OF INTERESTS

The authors declare that they have no conflict of interest.

ACKNOWLEDGEMENT

The authors hereby acknowledge the Research and Postgraduate Support Directorate and the Institute of Systems Science, Durban University of Technology, South Africa.

REFERENCE

[1] A. T. Doppalapudi, A. K. Azad, and M. M. K. Khan, "Advanced strategies to reduce harmful nitrogen-oxide emissions from biodiesel fueled engine," *Renewable and Sustainable Energy Reviews,* vol. 174, p. 113123, 2023/03/01/ 2023. Available: https://www.sciencedirect.com/science/article/pii/S1364032122010048

[2] P. Kurzawska, "Overview of Sustainable Aviation Fuels including emission of particulate matter and harmful gaseous exhaust gas compounds," *Transportation Research Procedia,* vol. 59, pp. 38-45, 2021/01/01/ 2021. https://www.sciencedirect.com/science/article/pii/S2352146521008565

[3] L. Zhang, R. Qin, N. Chai, H. Wei, Y. Yang, Y. Wang*, et al.*, "Optimum fertilizer application rate to ensure yield and decrease greenhouse gas emissions in rain-fed agriculture system of the Loess Plateau," *Science of The Total Environment,* vol. 823, p. 153762, 2022/06/01/ 2022. Available: https://www.sciencedirect.com/science/article/pii/S0048969722008543

[4] D. Konkol, E. Popiela, D. Skrzypczak, G. Izydorczyk, K. Mikula, K. Moustakas*, et al.*, "Recent innovations in various methods of harmful gases conversion and its mechanism in poultry farms," *Environmental Research,* vol. 214, p. 113825, 2022/11/01/ 2022. Available: https://www.sciencedirect.com/science/article/pii/S0013935122011525

[5] W. S. Ebhota and T.-C. Jen, "Fossil Fuels Environmental Challenges and the Role of Solar Photovoltaic Technology Advances in Fast Tracking Hybrid Renewable Energy System," *International Journal of Precision Engineering and Manufacturing-Green Technology,* vol. 7, pp. 97-117, 2020/01/01 2020. Available: https://doi.org/10.1007/s40684-019-00101-9

[6] FocusEconomics, "The World's Fastest Growing Economies," Barcelona, Spain16/02/2023 2022. Available: https://www.focus-economics.com/blog/fastest-growing-economies-in-the-world

[7] K.-Y. Show and D.-J. Lee, "Chapter 13 - Bioreactor and Bioprocess Design for Biohydrogen Production," in *Biohydrogen*, A. Pandey, J.-S. Chang, P. C. Hallenbecka, and C. Larroche, Eds., ed Amsterdam: Elsevier, 2013, pp. 317-337. Available: https://www.sciencedirect.com/science/article/pii/B9780444595553000131

[8] T. Laan and A. G. Maino, "Boom and Bust: The fiscal implications of fossil fuel phase-out in six large emerging economies," Canada2022. Available: https://www.iisd.org/publications/report/fossil-fuel-phase-out-briics-economies

[9] SDGs. (2019, 21/05/2022). *Goal 13: Take urgent action to combat climate change and its impacts*, The United Nations Sustainable Development Goals. Available: https://www.un.org/sustainabledevelopment/climate-change/

[10] UN, "Greening the Blue Report 2021: The UN System's Environmental Footprint and Efforts to Reduce It," The United Nations (UN) Environment Programme, Geneva2021. Available: www.greeningtheblue.org/reports/greening-blue-report-2021

[11] W. S. Ebhota, "Power accessibility, fossil fuel and the exploitation of small hydropower technology in sub-Saharan Africa," *International Journal of Sustainable Energy Planning and Management* vol. 19, 2019. Available: https://doi.org/10.5278/ijsepm.2019.19.3

[12] M. Shahbaz, C. Raghutla, K. R. Chittedi, Z. Jiao, and X. V. Vo, "The effect of renewable energy consumption on economic growth: Evidence from the renewable energy country attractive index," *Energy,* vol. 207, p. 118162, 2020/09/15/ 2020. Available: http://www.sciencedirect.com/science/article/pii/S036054422031269X

[13] S. A. R. Khan, Z. Yu, A. Belhadi, and A. Mardani, "Investigating the effects of renewable energy on international trade and environmental quality," *Journal of Environmental Management,* vol. 272, p. 111089, 2020/10/15/ 2020. Available: http://www.sciencedirect.com/science/article/pii/S0301479720310161

[14] J. Huang, W. Li, L. Guo, X. Hu, and J. W. Hall, "Renewable energy and household economy in rural China," *Renewable Energy,* vol. 155, pp. 669-676, 2020/08/01/ 2020. Available: http://www.sciencedirect.com/science/article/pii/S0960148120304845

[15] S. R. Sinsel, R. L. Riemke, and V. H. Hoffmann, "Challenges and solution technologies for the integration of variable renewable energy sources—a review," *Renewable Energy,* vol. 145, pp. 2271-2285, 2020/01/01/ 2020. Available: http://www.sciencedirect.com/science/article/pii/S0960148119309875

[16] H. Lucas, S. Fifita, I. Talab, C. Marschel, and L. F. Cabeza, "Critical challenges and capacity building needs for renewable energy deployment in Pacific Small Island Developing States (Pacific SIDS)," *Renewable Energy,* vol. 107, pp. 42-52, 2017/07/01/ 2017. Available: http://www.sciencedirect.com/science/article/pii/S0960148117300290

[17] C. Dondariya, D. Porwal, A. Awasthi, A. K. Shukla, K. Sudhakar, M. M. S.R, *et al.*, "Performance simulation of grid-connected rooftop solar PV system for small households: A case study of Ujjain, India," *Energy Reports,* vol. 4, pp. 546-553, 2018/11/01/ 2018. Available: https://www.sciencedirect.com/science/article/pii/S2352484718300647

[18] Fuzen. (2021, 03/05/2021). *List of solar PV design software tools*. Available: https://www.fuzen.io/solar-epc/list-of-solar-pv-design-software-tools/

[19] T. Khatib, A. Mohamed, and K. Sopian, "A Software Tool for Optimal Sizing of PV Systems in Malaysia," *Modelling and Simulation in Engineering,* vol. 2012, p. 969248, 2012/05/09 2012. Available: https://doi.org/10.1155/2012/969248

[20] Solar. (2022, 16/02/2022). *Solar energy is the fastest growing renewable energy source*. Available: https://quebecsolar.ca/solar-energy-is-the-fastest-growing-renewable-energy-source/

[21] M. Boxwell, *Solar Electricity Handbook, a Simple Practical Guide to Solar Energy-Designing and Installing Photovoltaic Solar Electric Systems*, 2 ed. London: Code Green Publishing, 2021.

[22] K. Lovegrove and M. Dennis, "Solar thermal energy systems in Australia," *International Journal of Environmental Studies,* vol. 63, pp. 791-802, 2006/12/01 2006. Available: https://doi.org/10.1080/00207230601047156

[23] S. Gerber, A. J. Rix, and M. J. Booysen, "Towards sustainable developing cities: A simplified forecasting model for sizing grid-tied PV using monthly electricity bills," *Sustainable Cities and Society,* vol. 54, p. 101994, 2020/03/01/ 2020. Available: https://www.sciencedirect.com/science/article/pii/S2210670719335358

[24] R. Othman and T. M. Hatem, "Assessment of PV technologies outdoor performance and commercial software estimation in hot and dry climates," *Journal of Cleaner Production,* vol. 340, p. 130819, 2022/03/15/ 2022. Available: https://www.sciencedirect.com/science/article/pii/S0959652622004577

[25] *DTU Energy. (27/04/2018). Solar Cells - the Three Generations*. Available: http://www.plasticphotovoltaics.org/lc/lc-solarcells/lc-introduction.html

[26] *Solar Facts and Advice. (2013, 21/04/2018). My Advice: Understand the Advantages, Disadvantages of Different Solar Cells and Who the Market Leaders Are*. Available: http://www.solar-facts-and-advice.com/solar-cells.html

[27] M. Fedkin and J. A. Dutton. (2020). *Solar Facts and Advice. (2013, 21/04/2018). Good Reasons Why Monocrystalline Solar Panels are the Industry Standard*. https://www.e-education.psu.edu/eme812/node/608

[28] E. Bisengimana, J. Zhou, M. Binama, and Y. Yuan, "Numerical investigation on the factors influencing the temperature distribution of photovoltaic/thermal (PVT) evaporator/condenser for heat pump systems," *Renewable Energy,* vol. 194, pp. 885-901, 2022/07/01/ 2022. https://www.sciencedirect.com/science/article/pii/S096014812200814X

[29] L. D. Jathar, S. Ganesan, U. Awasarmol, K. Nikam, K. Shahapurkar, M. E. M. Soudagar, *et al.*, "Comprehensive review of environmental factors influencing the performance of photovoltaic panels: Concern over emissions at various phases throughout the lifecycle," *Environmental Pollution,* vol. 326, p. 121474, 2023/06/01/ 2023. Available: https://www.sciencedirect.com/science/article/pii/S0269749123004761

[30] M. S. P. Moren and A. Korjenic, "Green buffer space influences on the temperature of photovoltaic modules: Multifunctional system: Building greening and photovoltaic," *Energy and Buildings,* vol. 146, pp. 364-382, 2017/07/01/ 2017. Available: https://www.sciencedirect.com/science/article/pii/S0378778817314007

[31] Energyfaculty.com. (28/04/2018). *Photovoltaic Energy Generation*. Available: https://energyfaculty.com/photovoltaic-energy-generation/

[32] M. Fedkin and J. A. Dutton. *Solar Facts and Advice. (2010, 21/04/2018). SunPower Solar Cells – The Most Efficient*. Available: http://www.solar-facts-and-advice.com/SunPower.html

[33] W. S. Ebhota and T.-C. Jen, "Photovoltaic solar energy: potentials and outlooks," presented at the ASME International Mechanical Engineering Congress and Exposition, Pittsburgh, Pennsylvania, USA, 2018. Available: http://dx.doi.org/10.1115/IMECE2018-86991

[34] M. A. Green, E. D. Dunlop, J. Hohl-Ebinger, M. Yoshita, N. Kopidakis, and X. Hao, "Solar cell efficiency tables (version 56)," *Progress in Photovoltaics: Research and Applications,* vol. 28, pp. 629-638, 2020. Available: https://onlinelibrary.wiley.com/doi/abs/10.1002/pip.3303

[35] Energy.gov, "Solar Energy Technologies Office: Cadmium Telluride," Office of Energy Efficiency & Renewable Energy, Washington DC2022. Available: https://www.energy.gov/eere/solar/cadmium-telluride

[36] ESMAP, "Global photovoltaic power potential by country," Energy Sector Management Assistance Program (ESMAP), World Bank, Washington DC2020. Available: https://www.worldbank.org/en/topic/energy/publication/solar-photovoltaic-power-potential-by-country

[37] Solargis. (2023, 15/05/2023). *Documentation - Methodology: Meteorological models and post-processing*. Available: https://solargis.com/docs/methodology/meteo-data

[38] S. Jouttijärvi, G. Lobaccaro, A. Kamppinen, and K. Miettunen, "Benefits of bifacial solar cells combined with low voltage power grids at high latitudes," *Renewable and Sustainable Energy Reviews,* vol. 161, p. 112354, 2022/06/01/ 2022. Available:

https://www.sciencedirect.com/science/article/pii/S1364032122002659

[39] S. Golroodbari, V. Fthenakis, and W. G. J. H. M. van Sark, "1.32 - Floating Photovoltaic Systems," in *Comprehensive Renewable Energy (Second Edition)*, T. M. Letcher, Ed., ed Oxford: Elsevier, 2022, pp. 677-702. Available: https://www.sciencedirect.com/science/article/pii/B9780128197271001746

[40] P. M. Rich, R. Dubayah, W. A. Hetrick, and S. C. Saving, "Using viewshed models to calculate intercepted solar radiation: applications in ecology," *American Society for Photogrammetry and Remote Sensing Technical Papers,* pp. 524-529, 1994. Available: http://professorpaul.com/publications/rich_et_al_1994_asprs.pdf

[41] P. Fu and P. M. Rich, "A geometric solar radiation model with applications in agriculture and forestry," *Computers and Electronics in Agriculture,* vol. 37, pp. 25-35, 2002/12/01/ 2002. Available: http://www.sciencedirect.com/science/article/pii/S0168169902001151

[42] ArcMap. (2020, 19/09/2021). *How solar radiation is calculated*. Available: https://desktop.arcgis.com/en/arcmap/10.3/tools/spatial-analyst-toolbox/how-solar-radiation-is-calculated.htm

[43] J. F. Orgill and K. G. T. Hollands, "Correlation equation for hourly diffuse radiation on a horizontal surface," *Solar Energy,* vol. 19, pp. 357-359, 1977/01/01/ 1977. Available: https://www.sciencedirect.com/science/article/pii/0038092X77900068

[44] D. G. Erbs, S. A. Klein, and J. A. Duffie, "Estimation of the diffuse radiation fraction for hourly, daily and monthly-average global radiation," *Solar Energy,* vol. 28, pp. 293-302, 1982/01/01/ 1982. Available: https://www.sciencedirect.com/science/article/pii/0038092X82903024

[45] L. Ashok Kumar, V. Indragandhi, and Y. Uma Maheswari, "Chapter 9 - PVSYST," in *Software Tools for the Simulation of Electrical Systems*, L. Ashok Kumar, V. Indragandhi, and Y. Uma Maheswari, Eds., ed: Academic Press, 2020, pp. 349-392. Available: https://www.sciencedirect.com/science/article/pii/B9780128194164000090

[46] M. E.-H. Dahmoun, B. Bekkouche, K. Sudhakar, M. Guezgouz, A. Chenafi, and A. Chaouch, "Performance evaluation and analysis of grid-tied large scale PV plant in Algeria," *Energy for Sustainable Development,* vol. 61, pp. 181-195, 2021/04/01/ 2021. Available: https://www.sciencedirect.com/science/article/pii/S0973082621000235

[47] E. de Freitas Moscardini Júnior and R. Rüther, "The influence of the solar radiation database and the photovoltaic simulator on the sizing and economics of photovoltaic-diesel generators," *Energy Conversion and Management,* vol. 210, p. 112737, 2020/04/15/ 2020. Available: https://www.sciencedirect.com/science/article/pii/S0196890420302752

[48] S. Sukumaran and K. Sudhakar, "Fully solar powered airport: A case study of Cochin International airport," *Journal of Air Transport Management,* vol. 62, pp. 176-188, 2017/07/01/ 2017. Available: https://www.sciencedirect.com/science/article/pii/S0969697717300297

[49] NREL. (2022, 08/09/2022). *Best Research-Cell Efficiency Chart*.The National Renewable Energy Laboratory, the U.S. Department of Energy, Office of Energy Efficiency and Renewable Energy, USA. Available: https://www.nrel.gov/pv/cell-efficiency.html

[50] M. Guo, H. Zang, S. Gao, T. Chen, J. Xiao, L. Cheng*, et al.*, "Optimal Tilt Angle and Orientation of Photovoltaic Modules Using HS Algorithm in Different Climates of China," *Applied Sciences,* vol. 7, p. 1028, 2017. Available: https://www.mdpi.com/2076-3417/7/10/1028

[51] K. Bakirci, "General models for optimum tilt angles of solar panels: Turkey case study," *Renewable and Sustainable Energy Reviews,* vol. 16, pp. 6149-6159, 2012/10/01/ 2012. Available: https://www.sciencedirect.com/science/article/pii/S1364032112004509

[52] M. H. Ibrahim and M. A. Ibrahim, "The Optimum PV Panels Slope Angle for Standalone System: Case Study in Duhok, Iraq," *IOP Conference Series: Materials Science and Engineering,* vol. 1076, p. 012004, 2021/02/01 2021. Available: http://dx.doi.org/10.1088/1757-899X/1076/1/012004

[53] D. D. Rooij. (2020, 13/06/2022). *Solar Panel Angle: how to calculate solar panel tilt angle?* , Sinovoltaics, Hong Kong. Available: https://sinovoltaics.com/learning-center/system-design/solar-panel-angle-tilt-calculation/

[54] J. Kern and I. Harris, "On the optimum tilt of a solar collector," *Solar Energy,* vol. 17, pp. 97-102, 1975/05/01/ 1975. Available: https://www.sciencedirect.com/science/article/pii/0038092X7590064X

[55] Heywood and H., "Operating experience with solar water heating.," *Journal of the Institution of Heating and Ventilation Engineers,* vol. 39, pp. 63-69, 1971.

[56] H. Hottel and B. Woertz, "Performance of flat-plate solar-heat collectors," *Trans. ASME (Am. Soc. Mech. Eng.); (United States),* vol. 64, pp. Medium: X; Size: Pages: 91 2009-12-16, 1942. Available: https://www.osti.gov/biblio/5052689

[57] G. O. G. Löf and R. A. Tybout, "Cost of house heating with solar energy," *Solar Energy,* vol. 14, pp. 253-278, 1973/02/01/ 1973. Available: https://www.sciencedirect.com/science/article/pii/0038092X73900947

[58] T. H. Stevens, "The economics of solar home heating systems for the southwest region," *The Journal of Energy and Development,* vol. 2, pp. 279-291, 1977. Available: http://www.jstor.org/stable/24806205

[59] H. K. Elminir, A. E. Ghitas, F. El-Hussainy, R. Hamid, M. M. Beheary, and K. M. Abdel-Moneim, "Optimum solar flat-plate collector slope: Case study for Helwan, Egypt," *Energy Conversion and Management,* vol. 47, pp. 624-637, 2006/03/01/ 2006. Available: https://www.sciencedirect.com/science/article/pii/S0196890405001342

[60] A. Awasthi, A. K. Shukla, M. M. S.R, C. Dondariya, K. N. Shukla, D. Porwal*, et al.*, "Review on sun tracking technology in solar PV system," *Energy Reports,* vol. 6, pp. 392-405, 2020/11/01/ 2020. Available: https://www.sciencedirect.com/science/article/pii/S2352484719304780

[61] J. Donev. (2023). *How to calculate solar PV panel orientation*. Available: https://energyeducation.ca/encyclopedia/Solar_panel_orientation#cite_note-RE1-3

[62] S. Memme and M. Fossa, "Maximum energy yield of PV surfaces in France and Italy from climate based equations for optimum tilt at different azimuth angles," *Renewable Energy,* vol. 200, pp. 845-866, 2022/11/01/ 2022. Available: https://www.sciencedirect.com/science/article/pii/S0960148122015129

[63] J. Yellott, "Utilization of Sun and Sky Radiation for Heating and Cooling of Building," *The Magazine of the Society of Air-Conditioning and Refrigerating Engineers of Korea,* vol. 4, pp. 309-325, 1975.

[64] IEC, "IEC 61724-1: Photovoltaic system performance monitoring," European Standard, Czech Republic2021. Available: https://www.en-standard.eu/bs-en-iec-61724-1-2021-photovoltaic-system-performance-monitoring/?gclid=CjwKCAjwysipBhBXEiwApJOcuxCdjII5ElNJb1Q27I-gCqsC5OmlLyp4qbueO2rIHIL4wU4lw22nehoC4lcQAvD_BwE

[65] R. A. T. Khan, M. F. Abbas, A. N. Khan, N. Ahmed, M. A. Qaisrani, and M. Assadi, "Performance assessment and root-cause analysis of a deteriorating On-Grid Industrial PV System for the identification of newly originating power degrading defect," *Energy for Sustainable Development,* vol. 76, p. 101306, 2023/10/01/ 2023. https://www.sciencedirect.com/science/article/pii/S0973082623001631

[66] B. Shiva Kumar and K. Sudhakar, "Performance evaluation of 10 MW grid connected solar photovoltaic power plant in India," *Energy Reports,* vol. 1, pp. 184-192, 2015/11/01/ 2015. Available: https://www.sciencedirect.com/science/article/pii/S2352484715000311

[67] D. A. Quansah, M. S. Adaramola, G. K. Appiah, and I. A. Edwin, "Performance analysis of different grid-connected solar photovoltaic (PV) system technologies with combined capacity of 20 kW located in humid tropical climate," *International Journal of Hydrogen Energy,* vol. 42, pp. 4626-4635, 2017/02/16/ 2017. Available: https://www.sciencedirect.com/science/article/pii/S0360319916310011

[68] W. S. Ebhota and P. Y. Tabakov, "Assessment of solar PV potential and performance of a household system in Durban North, Durban, South Africa," *Clean Technologies and Environmental Policy,* 2021/11/24 2021. Available: https://doi.org/10.1007/s10098-021-02241-6

[69] M. R. Patel. (2005). *Wind and Solar Power Systems: Design, Analysis, and Operation (2nd ed.)*. Available: https://doi.org/10.1201/9781420039924

[70] A. N. K. Marc, "Measuring Solar Irradiance for Photovoltaics," in *Solar Radiation*, A. Mohammadreza, Ed., ed Rijeka: IntechOpen, 2022, p. Ch. 2. Available: https://doi.org/10.5772/intechopen.105580

[71] Weatherspark. (14/06/2022). *Climate & Weather Averages in Durban, South Africa*, Weather Spark, Cedar Lake Ventures, Inc. Minneapolis, United States. Available: https://weatherspark.com/s/96783/1/Average-Summer-Weather-in-Durban-South-Africa

[72] B. Amiri, A. M. Gómez-Orellana, P. A. Gutiérrez, R. Dizène, C. Hervás-Martínez, and K. Dahmani, "A novel approach for global solar irradiation forecasting on tilted plane using Hybrid Evolutionary Neural Networks," *Journal of Cleaner Production,* vol. 287, p. 125577, 2021/03/10/ 2021. Available: https://www.sciencedirect.com/science/article/pii/S0959652620356237

[73] K. Bouchouicha, M. A. Hassan, N. Bailek, and N. Aoun, "Estimating the global solar irradiation and optimizing the error estimates under Algerian desert climate," *Renewable Energy,* vol. 139, pp. 844-858, 2019/08/01/ 2019. Available: https://www.sciencedirect.com/science/article/pii/S0960148119302253

[74] A. Takilalte, S. Harrouni, M. R. Yaiche, and L. Mora-López, "New approach to estimate 5-min global solar irradiation data on tilted planes from horizontal measurement," *Renewable Energy,* vol. 145, pp. 2477-2488, 2020/01/01/ 2020. Available: https://www.sciencedirect.com/science/article/pii/S0960148119311851

[75] Q. Lagarde, B. Beillard, S. Mazen, M.-S. Denis, and J. Leylavergne, "Performance ratio of photovoltaic installations in France: Comparison between inverters and micro-inverters," *Journal of King Saud University - Engineering Sciences,* 2021/11/27/ 2021. Available: https://www.sciencedirect.com/science/article/pii/S1018363921001677

[76] B. Hashemi, S. Taheri, A.-M. Cretu, and E. Pouresmaeil, "Systematic photovoltaic system power losses calculation and modeling using computational intelligence techniques," *Applied Energy,* vol. 284, p. 116396, 2021/02/15/ 2021. Available: https://www.sciencedirect.com/science/article/pii/S0306261920317670

[77] S. I. Sulaiman, H. A. Majid, and Z. Othman, "Loss of load probability minimization for stand-alone photovoltaic system using elephant herding optimization," *Energy Reports,* vol. 8, pp. 1038-1044, 2022/11/01/ 2022. Available: https://www.sciencedirect.com/science/article/pii/S2352484722011246

[78] M.-H. Tan, T.-K. Wang, C.-W. Wong, B.-H. Lim, T.-K. Yew, W.-C. Tan, *et al.*, "Optimization Study of Parasitic Energy Losses in Photovoltaic System with Dual-Axis Solar Tracker Located at Different Latitudes," *Energy Procedia,* vol. 158, pp. 302-308, 2019/02/01/ 2019. Available: https://www.sciencedirect.com/science/article/pii/S1876610219301031

[79] C.-Y. Park, S.-H. Hong, S.-C. Lim, B.-S. Song, S.-W. Park, J.-H. Huh, *et al.*, "Inverter Efficiency Analysis Model Based on Solar Power Estimation Using Solar Radiation," *Processes,* vol. 8, p. 1225, 2020. Available: https://www.mdpi.com/2227-9717/8/10/1225

[80] W. S. Ebhota and P. Y. Tabakov, "Influence of photovoltaic cell technologies and elevated temperature on photovoltaic system performance," *Ain Shams Engineering Journal,* vol. 14, p. 101984, 2023/07/01/ 2023. Available: https://www.sciencedirect.com/science/article/pii/S2090447922002957

[81] ECOFLOW. (2032, 25/10/2023). *The Impact of Temperature on Solar Panel Efficiency: How Heat Affects Your Solar Energy System*. Available: https://blog.ecoflow.com/au/effects-of-temperature-on-solar-panel-efficiency/

[82] W. S. Ebhota and P. Y. Tabakov, "Assessment and performance analysis of roof-mounted crystalline stand-alone photovoltaic (SAPV) system at selected sites in South Africa," *Bulletin of the National Research Centre,* vol. 46, p. 236, 2022/08/27 2022. Available: https://doi.org/10.1186/s42269-022-00929-3

[83] W. S. Ebhota and P. Y. Tabakov, "Assessment of solar photovoltaic potential of selected site locations in cities across sub-Saharan Africa," *Energy Systems,* 2023/10/16 2023. Available: https://doi.org/10.1007/s12667-023-00625-9